

# [CpNi(diselenolene)] Neutral Radical Complexes: Electron Paramagnetic Resonance and Density Functional Theory Investigations

Philippe Grosshans,<sup>†</sup> Prashant Adkine,<sup>†</sup> Helena Sidorenkova,<sup>†</sup> Mitsuhiro Nomura,<sup>‡</sup> Marc Fourmigué,<sup>\*,‡</sup> and Michel Geoffroy<sup>\*,†</sup>

Department of Physical Chemistry, 30 quai Ernest Ansermet, University of Geneva, 1211 Geneva, Switzerland, and Sciences Chimiques de Rennes, Université de Rennes 1, UMR CNRS 6226, Campus de Beaulieu, 35042 Rennes, France

Received: January 21, 2008

<sup>77</sup>Se-enriched CpNi(bds) (bds = 1,2-benzenediselenolate), has been synthesized and its *g* tensor and <sup>77</sup>Se hyperfine tensors have been obtained from its frozen solution electron paramagnetic resonance (EPR) spectrum. These parameters are consistent with those calculated by density functional theory (DFT); it is shown that 10% of the spin is localized on each selenium and that the direction associated to the maximum <sup>77</sup>Se couplings is aligned along the *g*<sub>min</sub> direction, perpendicular to the Ni(bds) plane. EPR measurements and DFT calculations are also carried out on the <sup>77</sup>Se enriched complex CpNi(dsit) as well on the two dithiolene analogues CpNi(bdt) and CpNi(dmit). The optimized structures of the isolated CpNi(bds) and CpNi(bdt) complexes have been used to generate the idealized dimers (bds)NiCp···CpNi(bds) and (bdt)NiCp···CpNi(bdt) characterized by Cp···Cp overlap. The exchange parameters *J* calculated at the DFT level for these systems are in reasonable accord with the experimental values. The influence of the geometry of the dimer on its magnetic properties is assessed by calculating the variation of *J* as a function of the relative orientation of the two Ni(diselenolene) or Ni(dithiolene) planes.

## Introduction

Nickel dithiolenes constitute an important class of complexes that can easily give rise to paramagnetic intermediates. This property, potentially useful in material sciences, has stimulated many electron paramagnetic resonance (EPR) investigations; this was the case, for example, for a large variety of monoanionic, formally Ni<sup>III</sup>, d<sup>7</sup>, Ni bis-dithiolene complexes compounds.<sup>1–3</sup> Dithiolene complexes, in which Ni is coordinated to a cyclopentadienyl ring, have been considerably less studied.<sup>4,5</sup> It has been realized only recently that CpNi(dithiolene), as well as their diselenolene analogues, present specific properties that are particularly attractive for the elaboration of magnetic materials. These 17-electron complexes are robust, neutral and paramagnetic.<sup>6</sup> The absence of counterion in the crystal matrix facilitates interaction between the complexes and is quite appropriate for exchange couplings between the paramagnetic centers, as confirmed for every of these complexes,<sup>4–7</sup> where extended one-dimensional or three-dimensional magnetic structures were observed, such as uniform spin chains, alternated spin chains or ordered antiferromagnets. On the other hand, for CpNi(bdt), the variation of the temperature dependence of the magnetic susceptibility clearly reveals the presence of antiferromagnetic interactions that cannot be ascribed to an extended set of interactions. For these systems indeed, the crystal structure shows that, in contrast with other CpNi(dithiolene) complexes, the intermolecular metal–sulfur or sulfur–sulfur distances are rather large and suggest that the origin of the exchange coupling lies in an unexpected bimolecular interaction between the

cyclopentadienyl rings of two CpNi(bdt) complexes facing each other through a Cp···Cp interaction.<sup>4</sup> A similar behavior was also recently observed in the CpNi(adt) complex where the face-to-face Cp···Cp interaction of two CpNi(adt) complexes (Chart 1) was held for responsible for the large antiferromagnetic interaction measured in this complex.<sup>8</sup> Calculation of the spin densities on the Cp ring indicated indeed that up to 20% spin density was indeed delocalized on the Cp ring, in CpNi(bdt)<sup>4</sup> as well as in CpNi(adt).<sup>8</sup>

However, confirmation of this hypothesis of a strong antiferromagnetic interaction through an intermolecular Cp···Cp interaction requires to experimentally accessing the exact spin delocalization in the isolated complex. Direct information about the spin densities can, *a priori*, be obtained from hyperfine interactions; for CpNi(dithiolene) complexes, however, no proton coupling is resolved on the EPR spectra and, due to the poor abundance of its magnetic isotope (<sup>33</sup>S, *I* = 3/2, natural abundance = 0.75%), no sulfur coupling can be detected. Therefore, substitution of sulfur atoms by selenium atoms appears to be the most pertinent method: <sup>77</sup>Se has a natural abundance of 7.3% and its spin number is only 1/2. Unfortunately, the large line width of the EPR signals of CpNi(bds) precluded the detection of the corresponding satellite lines. We therefore decided to enrich some CpNi(diselenolene) complexes with <sup>77</sup>Se isotope and to determine their <sup>77</sup>Se couplings and *g* tensor from their frozen solution spectra. In this study, we report the preparation and the EPR study of <sup>77</sup>Se enriched CpNi(bds) and CpNi(dsit), (Chart 2), as well as the measured *g* values for the corresponding dithiolene complexes CpNi(bdt) and CpNi(dmit).

To test the ability of density functional theory (DFT) calculations to predict the structure of the isolated complexes, the experimental *g* and <sup>77</sup>Se coupling tensors are compared with

\* Corresponding author. Tel.: (+) 41 22 379 65 52. Fax: (+) 41 22 379 61 03. E-mail: michel.geoffroy@chiphy.unige.ch.

<sup>†</sup> University of Geneva.  
<sup>‡</sup> Université de Rennes 1.

## CHART 1

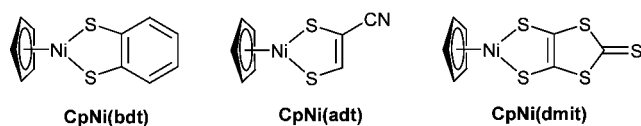


## CHART 2



those predicted by this theory and the calculated exchange coupling constant  $J$  resulting from the interaction between two CpNi(bds) or two CpNi(bdt) complexes is compared with the value previously obtained from magnetic measurements. An important objective of these investigations is also to point to the dependence of the magnetic properties of (bds)NiCp...CpNi(bds) or (bdt)NiCp...CpNi(bdt) on the relative orientation of the two monomers.

## Experimental Methods

**Synthesis. General Details.** All reactions were carried out under an argon atmosphere by means of standard Schlenk techniques. All solvents for chemical reactions were dried and distilled by Na–benzophenone (for toluene) or CaH<sub>2</sub> (for methanol) before use. Metallic <sup>77</sup>Se was obtained from Eurisotop (Saclay, France), a subsidiary of Cambridge Isotope Laboratories, Inc.

**Synthesis of <sup>77</sup>Se-Enriched (NEt<sub>4</sub>)<sub>2</sub>[Zn(dsit)<sub>2</sub>].** A 1.6 M solution of *n*-butyllithium in hexane (0.44 mL, 0.7 mmol) was slowly added from a syringe to a stirred solution of diisopropylamine (0.09 mL, 0.65 mmol) in 2 mL of dry THF under –78 °C. After 1 h, the THF solution (3 mL) of vinylene trithiocarbonate (44 mg, 0.33 mmol) was added over 15 min. The reaction mixture was allowed to react under –78 °C for 3 h. The solid <sup>77</sup>Se (48 mg, 0.62 mmol, red form) was directly added into the reaction mixture in one portion. The vigorously stirred solution was allowed to warm up to room temperature, and reacted for 18 h. Then a dark-red solution was obtained. The solvent was evaporated under reduced pressure under argon atmosphere. A methanol solution (3 mL) containing tetraethylammonium bromide (137 mg, 0.65 mmol) and zinc chloride (45 mg, 0.33 mmol) was added into the residue. Then a red precipitate was rapidly formed. After stirring for 30 min, water (10 mL) was added to precipitate the salt. The cloudy solution was filtered and the red solid obtained was washed with water. The red solid was dried under reduced pressure. A 211 mg amount of the crude <sup>77</sup>Se<sub>4</sub>–(NEt<sub>4</sub>)<sub>2</sub>[Zn(dsit)<sub>2</sub>] containing <sup>77</sup>Se-rich isotope was obtained. This product might include some impurities (e.g., remaining elemental <sup>77</sup>Se and vinylene trithiocarbonate), but it can be used directly for the next reaction.

**Synthesis of <sup>77</sup>Se-Enriched [CpNi(dsit)].** The crude <sup>77</sup>Se<sub>4</sub>–(NEt<sub>4</sub>)<sub>2</sub>[Zn(dsit)<sub>2</sub>] (211 mg) with <sup>77</sup>Se and [Cp<sub>2</sub>Ni](BF<sub>4</sub>) (130 mg, 0.47 mmol) were reacted in refluxing methanol for 2 h. <sup>77</sup>Se<sub>2</sub>–[CpNi(dsit)] was obtained in 20% overall yield based on elemental <sup>77</sup>Se. HR-Mass (MALDI<sup>+</sup>) Calcd for C<sub>8</sub>H<sub>5</sub>NiS<sub>3</sub><sup>77</sup>Se<sub>2</sub>: 408.7305. Found: 408.7270.

**Synthesis of <sup>77</sup>Se-Enriched (PPh<sub>4</sub>)<sub>2</sub>[Zn(bds)<sub>2</sub>].** Solid sodium (11.9 mg, 0.49 mmol, 1 equiv) and <sup>77</sup>Se (37 mg, 0.48 mmol, 1 equiv) were weighed under argon in a glovebox in a small test tube, DMF (1 mL) was added, and the mixture was warmed to 100 °C for 2 h. *o*-Dibromobenzene (38 μL, 0.32 mmol, 0.5 equiv)

was added directly in the test tube and the mixture was stirred at 140 °C for 40 h. The mixture was then cooled to room temperature, centrifuged (3 × 5 min at 5000 t/min) and washed with MeOH (3 × 2 mL) to give an orange solid (32%). NaBH<sub>4</sub> solid (6.5 equiv) was added to a suspension of this poly(*o*-diselenobenzene) (2 equiv) in MeOH (2 mL) at 0 °C and stirred for 1 h. ZnBr<sub>2</sub> (1 equiv) was then added to the solution, and after 1 h at 0 °C, PPh<sub>4</sub>Br (1 equiv) was added. The mixture was stirred at room temperature for 2 h to give an orange precipitate that was centrifuged (3 × 5 min at 5000 t/min) and washed with MeOH (3 × 2 mL) to give an orange-brown solid (185 mg, 64%). This crude product was used without further purification in the next step.

**Synthesis of <sup>77</sup>Se-Enriched [CpNi(bds)].** The crude <sup>77</sup>Se-enriched [PPh<sub>4</sub>]<sub>2</sub>[Zn(bds)<sub>2</sub>] prepared above was treated under argon with (Cp<sub>2</sub>Ni)BF<sub>4</sub> (132.3 mg, 0.48 mmol, 2 equiv) in dry MeOH (5 mL) and warmed to reflux for 2.5 h. After evaporation, the solid is taken in CH<sub>2</sub>Cl<sub>2</sub>/cyclohexane 1:1 and chromatographed on silica gel to afford the title compound as a dark solid in low yield (15 mg, 16%).

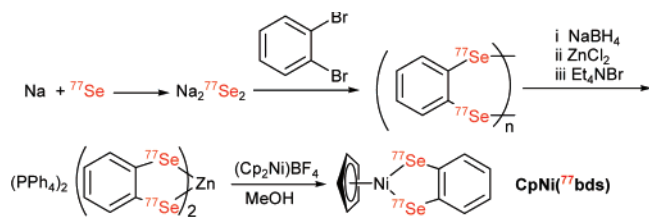
**EPR.** Measurements were carried out with a Bruker 300 spectrometer (X-band, 100 kHz field modulation). Frozen solution spectra were obtained by very rapidly cooling down the solution to avoid the formation of small crystallites. Frozen solution spectra have been simulated with the XSophe-Xepr-View computer simulation software<sup>9</sup> or with a program written in our laboratory that uses the Levenberg–Marquardt algorithm.<sup>10</sup>

**Calculations.** Geometries of the isolated complexes were optimized with no constraint using the Gaussian 03 package<sup>11</sup> and the hybrid functional B3LYP.<sup>12</sup> The standard 6-311G\*<sup>13</sup> basis set was used for H, C, S, and Se together with the ECP Stevens–Basch–Krauss basis (SBK)<sup>14</sup> for Ni. Energy minima were confirmed by frequencies analysis. The  $g$  tensors and the <sup>77</sup>Se hyperfine tensors of these complexes were obtained with the B3LYP functional, at the optimized geometries. Three sets of calculations were performed to predict these properties: (1) by using the Gaussian 03 program with the aug-cc-pVDZ basis set for H, C, S, Se atoms<sup>15</sup> and SBK for Ni (set a); (2) by using the ORCA program<sup>16</sup> with the aug-cc-pVDZ for H, C, S, Se atoms and the all-electron Gaussian basis sets triple- $\zeta$  quality TZV<sup>17</sup> for Ni (set b); (3) by using the basis set mentioned for set b together with the scalar relativistic zeroth-order regular approximation program (ZORA)<sup>18,19</sup> implemented in ORCA (set c). The exchange coupling parameter  $J$  has been calculated for the “dimeric” species with the ORCA program using the basis sets mentioned for set b. To assess the role of the functional on the calculated value of  $J$ , several types of functionals have been used for the calculations of this parameter: hybrid (B1LYP, B3LYP, PBE0<sup>20</sup>), generalized gradient approximation (GGA) (BP86, PBE, RPBE, BLYP) and local density approximation (LDA). The variation of  $J$  as a function of the dihedral angle SeNiNiSe has been calculated with the BP86 functional. The GaussView program has been used for the representation of molecules and orbitals.

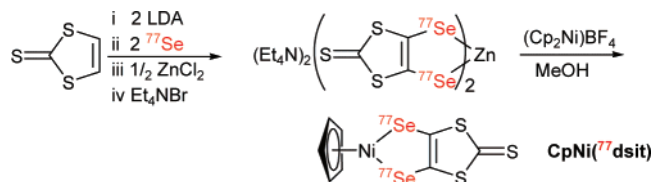
## Results

**<sup>77</sup>Se Enrichment of CpNi(diselenolene).** The syntheses of non-<sup>77</sup>Se-enriched diselenolene complexes have been published,<sup>4,21,22</sup> and they implied the reaction of nickel diselenolene complexes, [Ni(bds)<sub>2</sub>]<sup>0</sup> or PhSb(dsit) with, respectively, Cp<sub>2</sub>Ni or (Cp<sub>2</sub>Ni)BF<sub>4</sub>. However, to be able to carry these reactions with the highest yields on the minimal quantities imposed by the availability of the <sup>77</sup>Se isotope, we have developed a novel

## SCHEME 1



## SCHEME 2



preparation based on the reaction of the stable and easily available zinc bis-dithiolene or diselenolene complexes with (Cp<sub>2</sub>Ni)BF<sub>4</sub>. This reaction was first perfected for the synthesis of CpNi(dmit) from (Et<sub>4</sub>N)<sub>2</sub>[Zn(dmit)<sub>2</sub>] and (Cp<sub>2</sub>Ni)BF<sub>4</sub>, affording CpNi(dmit) in 70% yield. The dsit complex, CpNi(dsit), was similarly obtained from (Et<sub>4</sub>N)<sub>2</sub>[Zn(dsit)<sub>2</sub>] and (Cp<sub>2</sub>Ni)BF<sub>4</sub> in 56% yield under the same conditions (2h reflux in MeOH). Based on these strong improvements, it was therefore possible to consider the preparation of the <sup>77</sup>Se-enriched CpNi(<sup>77</sup>bds) and CpNi(<sup>77</sup>dsit), as outlined in Schemes 1 and 2, respectively.

**EPR Results.** The X-band EPR spectrum obtained at room temperature with a solution of CpNi(bdt) in THF exhibits a single line centered around  $g = 2.05$ , with a line width of  $\sim 10$  G. A single line is also observed with non-enriched diselenolene complexes CpNi(bds) or CpNi(dsit); in these cases, however, the  $g$  value is around 2.09 and the line width is close to 25 G. With the <sup>77</sup>Se-enriched compounds, the line width slightly increases, but no hyperfine coupling is resolved.

As shown by its frozen solution spectrum (Figure 1a), the  $g$  tensor of CpNi(bdt) is axial with  $g_{\perp} < g_{\parallel}$ . The spectrum obtained with CpNi(bds) (Figure 1b) exhibits some departure from axial symmetry. The  $g$  tensors of the two complexes have been determined by a simulation/optimization process; the resulting principal values are given in Table 1 together with the values measured for CpNi(dmit) and CpNi(dsit). For these complexes, the anisotropy ( $g_{\max} - g_{\min}$ ) is around 0.10; as expected from the room-temperature spectra, the average value for the dithiolene compounds is slightly smaller than for the diselenolene complex.

Enrichment of CpNi(bds) with <sup>77</sup>Se causes a drastic modification of its EPR response: a well-resolved hyperfine structure is now observed on the frozen solution spectrum (Figure 2a). A similar modification is observed when CpNi(dsit) is enriched in <sup>77</sup>Se (see Figure 2b).

The spin Hamiltonian used for the simulation of the CpNi(<sup>77</sup>bds) spectrum takes the  $g$  tensor and the hyperfine tensors  $T$  with two <sup>77</sup>Se nuclei into account. The  $g$  tensor is, of course, practically identical to the tensor measured for the non-enriched compound. The two <sup>77</sup>Se  $T$  tensors exhibit a pronounced axial symmetry, they have the same principal values and their <sup>77</sup>Se  $T_{\parallel}$  are aligned along the  $g_{\min}$  direction. The spectra are not very sensitive to the orientation of the “perpendicular” eigenvectors; the very good simulation shown in Figure 2a was performed with  $T_{\perp 1}$  (56 MHz), making an angle of 20° with  $g_{\max}$ . The signs of the hyperfine couplings cannot be directly determined from the spectra. However, a combination that assumes the sign

of  $T_3 = T_{\max}$  is opposite to the sign of  $T_1$  and  $T_2$  leads to the smallest absolute value for the isotropic coupling constant ( $A_{\text{iso}} \sim 26$  MHz); such a small value, together with the large line width of the signal, explains the absence of any hyperfine splitting on the liquid-phase spectrum. Accordingly, with the DFT results (*vide infra*), the combination leading to a positive isotropic coupling constant has been retained. The resulting experimental <sup>77</sup>Se isotropic and anisotropic coupling constants are reported in Table 1 together with those measured for CpNi(<sup>77</sup>dsit).

**DFT Results on Isolated Complexes.** Structure optimizations show that, in accord with preliminary calculations on CpNi(bdt),<sup>4</sup> the Ni(bdt) and Ni(bds) moieties are planar and oriented perpendicular to the Cp ring, in good accordance with the crystal structures.<sup>4</sup> Bond angles and torsion angles agree with those measured by X-ray diffraction; nevertheless, the Cp $\cdots$ Ni distances obtained by DFT are slightly larger than those measured in the crystal (Cp $\cdots$ Ni distances (Å): CpNi(bdt), 1.785 (DFT), 1.721 (crystal); CpNi(bds), 1.789 (DFT), 1.718 (crystal)).

Several recent reports have shown that the DFT method is now able to predict not only the hyperfine couplings but also the  $g$  tensors with a good accuracy.<sup>23–26</sup> The  $g$  tensors, obtained with the basis sets mentioned as sets a, b, c in the experimental section, are given in Table 2. For the four complexes, the  $g_{\min}$  eigenvector is oriented perpendicular to the Ni-containing ring ( $z$ -axis), and the two other principal directions are oriented parallel and perpendicular to the chalcogen–chalcogen direction of this ring (Figure 3).

For CpNi(<sup>77</sup>bds) and CpNi(<sup>77</sup>dsit), the three calculation sets (sets a, b, c), lead to the <sup>77</sup>Se hyperfine coupling constants shown in Table 2. For each complex, the two <sup>77</sup>Se  $A_{\text{iso}}$  constants are practically equal as well as the corresponding anisotropic coupling constants <sup>77</sup>Se  $\tau_{\text{aniso}}$ . The two <sup>77</sup>Se dipolar tensors have their maximum component ( $\tau_{\max}$ ) aligned along the  $g_{\min}$  direction ( $z$ -axis); the minimum component ( $\tau_1$ ) makes an angle of  $\sim 12^\circ$  with the corresponding Se–Ni bond direction.

**DFT Results on Interacting Complexes.** Recently, several reports have shown that the broken symmetry approach proposed by Noodleman<sup>27,28</sup> leads to very satisfactory predictions of the exchange coupling parameter  $J$ .<sup>29–33</sup> In this method,  $J$  is given by  $J_N = [E_{\text{HS}} - E_{\text{BS}}]/S^2_{\max}$ , where  $E_{\text{HS}}$  corresponds to the energy of the triplet (high-spin state) and  $E_{\text{BS}}$  to the energy of the singlet (low-spin state, where the spin-up electron quasi localizes on the first monomer and the spin-down electron quasi localizes on the second one) calculated in the broken symmetry unrestricted formalism. Another equation for  $J$  was proposed by Yamaguchi<sup>34</sup> ( $J_Y = [E_{\text{HS}} - E_{\text{BS}}]/[\langle S^2 \rangle_{\text{HS}} - \langle S^2 \rangle_{\text{BS}}]$ ). Although this DFT–BS method has been criticized,<sup>35</sup> it enables us to calculate our rather large system, (bds)NiCp $\cdots$ CpNi(bds) without having to approximate it to a simpler model.

First, the value of  $J$  has been calculated for the idealized dimer shown in Figure 4. In this system each CpNi(bds) “monomer” adopts the geometry optimized for the isolated complex (Ni $\cdots$ Cp distance = 1.789 Å). To mimic the crystal structure, the two monomers are related by a rotation of  $2(2\pi/5)$  around the  $x$ -axis, oriented perpendicular to the two Cp rings and bearing the two nickel atoms and the centers of the two cyclopentadienes; this leads to SeNiNiSe torsion angles equal to  $\sim 36^\circ$ , and in the real system two slightly different values are found for these angles: 31.2° and 24.8°. The distance between the two cyclopentadiene rings is equal to 3.37 Å as measured in the crystal.

The  $J_N$  and  $J_Y$  values calculated for this idealized dimer by using various functionals are reported in Table 3 together with

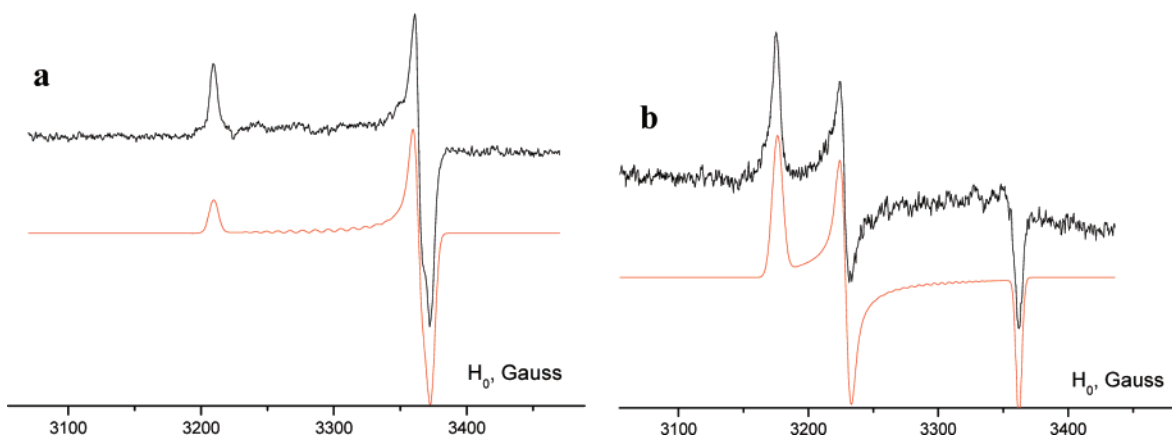


**Figure 1.** Experimental (top) and simulated (bottom) EPR spectra obtained at 77 K with a THF solution of CpNi(bdt) (a) and CpNi(bds) (b).

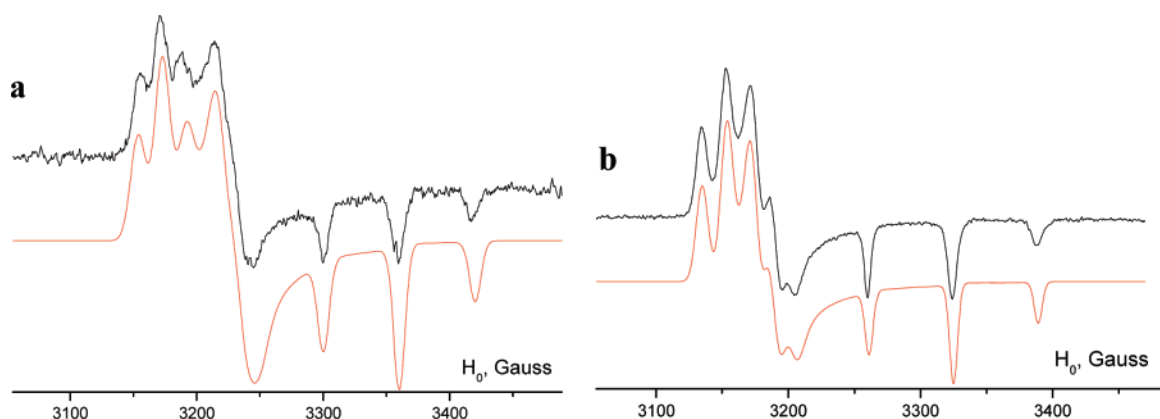


**Figure 2.** Experimental (top) and simulated (bottom) EPR spectra obtained at 77 K with a THF solution of  $^{77}\text{Se}$  enriched CpNi( $^{77}\text{bds}$ ) (a) and CpNi( $^{77}\text{dsit}$ ) (b).

**TABLE 1: Experimental EPR Tensors**

complex	$g$ tensor				$^{77}\text{Se}$ coupling tensor (MHz)			$^{77}\text{Se}$ $\tau_{\text{aniso}}$ (MHz)			$^{77}\text{Se}$ $A_{\text{iso}}$ (MHz)
	$g_1$	$g_2$	$g_3$	$g_{\text{av}}$	$T_1$	$T_2$	$T_3$	$\tau_1$	$\tau_2$	$\tau_3$	
CpNi(bdt)	2.121	2.024	2.018	2.054							
CpNi( $^{77}\text{bds}$ )	2.146	2.110	2.028	2.095	(-) $56$	(-) $33$	(+) $168$	(-) $82$	(-) $59$	(+) $142$	(+) $26$
CpNi(dmit)	2.096	2.028	2.014	2.046							
CpNi( $^{77}\text{dsit}$ )	2.161	2.137	2.050	2.116	(-) $59$	(-) $37$	(+) $188$	(-) $90$	(-) $68$	(+) $157$	(+) $31$

the values predicted for the geometry directly obtained from the crystal structure (Ni $\cdots$ Cp distance = 1.7 Å, angle between the Cp mean planes = 4.17°).

To assess the dependence of  $J$  with the topology of the “dimer”, we have also calculated the variation of this parameter as a function of the dihedral angle  $\xi$  formed by the two diselenolene or dithiolenes planes. The resulting curves, obtained for (bds)NiCp $\cdots$ CpNi(bds) by rotating one of the two Ni-(diselenolene) units around its symmetry axis and by keeping fixed the two cyclopentadienyl rings, are shown in Figure 5a. A similar variation is obtained by rotating one of the two CpNi-(diselenolene) complexes around this axis. The angular dependence of  $E_{\text{HS}}$  (triplet energy) and of  $E_{\text{BS}}$  (singlet energy) is reported in Figure 5b.

## Discussion

The large size of the studied complexes as well as the presence of several atoms with a high spin-orbit coupling constant (one Ni, two or five chalcogens) is not particularly favorable to an accurate calculation of the  $g$  tensor. As shown

by Table 2, this difficulty is reflected by the incidence of the choice of the basis set on the calculated data. Nevertheless, most of the  $g$  characteristics measured on the spectra are reproduced by DFT: the  $g_{\text{average}}$  values, rather close to the experimental ones, are larger for the diselenolenes than for the dithiolenes and the calculated anisotropies ( $g_{\text{max}} - g_{\text{min}}$ ) are consistent with EPR measurements.

The spin delocalization on the two selenium atoms can be roughly estimated by comparing the experimental  $^{77}\text{Se}$  couplings with the atomic constants.<sup>36</sup> This leads, for CpNi( $^{77}\text{bds}$ ), to a very small spin density in the s-orbitals of Se ( $\rho_s = 26/20120 = 0.1\%$ ) and to an appreciable p-character ( $\rho_p = 142/982 = 14\%$ ). Similar values are found for CpNi( $^{77}\text{dsit}$ ): ( $\rho_s = 0.1\%$ ,  $\rho_p = 16\%$ ). The DFT calculations confirm these results: for the two Ni selenolene complexes, the Fermi contact interaction, probably due to inner shell polarization, is small and agrees with the  $A_{\text{iso}}$  value obtained from the frozen solution spectra using the pertinent sign combination (*vide supra*); the maximum anisotropic coupling component  $\tau_{\text{max}}$  is practically equal to the experimental value. Consistent with the EPR results, for each

TABLE 2: Calculated  $g$  and  $^{77}\text{Se}$ -coupling Tensors

basis set	$g$ tensor				$^{77}\text{Se}-\tau_{\text{aniso}}$ (MHz)			$^{77}\text{Se}$ $A_{\text{iso}}$ (MHz)	
	$g_1$	$g_2$	$g_3$	$g_{\text{av}}$	$\tau_2$	$\tau_1$	$\tau_{\text{max}}$		
CpNi(bdt)	set a	2.1156	2.0442	2.0318	2.0638				
	set b	2.1119	2.0462	2.0245	2.0608				
	set c	2.1225	2.0442	2.0300	2.0655				
CpNi(bds)	set a	2.1383	2.1103	2.0480	2.0988	-109	-25	+135	+23
	set b	2.1506	2.1433	2.0402	2.1113	-102	-40	+142	+29
	set c	2.1535	2.1338	2.0489	2.1123	-94	-31	+125	+21
CpNi(dmit)	set a	2.0754	2.0574	2.0129	2.0485				
	set b	2.0703	2.0554	2.0095	2.0450				
	set c	2.0799	2.0554	2.0131	2.0482				
CpNi(dsit)	set a	2.1413	2.1167	2.0309	2.0963	-106	-55	+161	+11
	set b	2.1812	2.1155	2.0234	2.1067	-101	-66	+167	+26
	set c	2.1660	2.1262	2.0309	2.1077	-93	-55	+147	+19

<sup>a</sup> Set a, G03, B3LYP, basis: C, H, S, Se, aug-cc-pVDZ; Ni, SBK. Set b, ORCA, B3LYP, basis: C, H, S, Se, aug-cc-pVDZ; Ni, TZV. Set c, ORCA, B3LYP, basis: C, H, S, Se, aug-cc-pVDZ; Ni, TZV, ZORA.

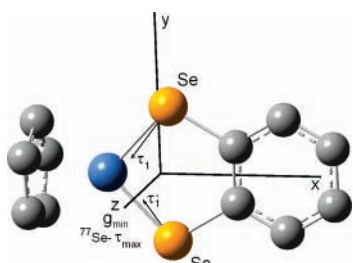


Figure 3. Orientation of the  $g_{\text{min}}$  and  $^{77}\text{Se}$   $\tau_{\text{max}}$  principal directions for CpNi(bds).

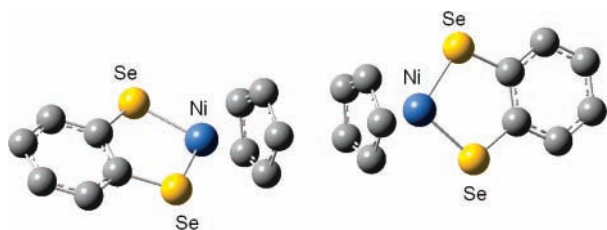


Figure 4. Idealized dimer formed by two CpNi(bds) units.

TABLE 3: Calculated<sup>a</sup>  $J$  ( $\text{cm}^{-1}$ ) Values for the Dimeric Structures of CpNi(bdt) and CpNi(bds)

	(CpNi(bdt)) <sub>2</sub>				(CpNi(bds)) <sub>2</sub>			
	crystal structure		idealized structure		crystal structure		idealized structure	
	$J_N$	$J_Y$	$J_N$	$J_Y$	$J_N$	$J_Y$	$J_N$	$J_Y$
LDA	-350	-282	-317	-257	-394		-371	
GGA								
BP86	-239	-213	-215	-192	-270	-237	-252	-222
PBE	-237	-211	-212	-190	-266	-234	-248	-220
RPBE	-217	-196	-192	-175	-242	-217	-224	-202
BLYP	-253	-223	-225	-200	-286	-248	-265	-232
hybrid								
B1LYP	-78	-77	-67	-66	-83	-83	-73	-72
B3LYP	-89	-88	-80	-79	-99	-97	-92	-90
PBE0	-71	-70	-61	-60	-76	-75	-66	-65
exptl					-313			

<sup>a</sup> ORCA, aug-cc-pVDZ basis sets for H, C, S, Se and TZV for Ni.

complex, the two selenium atoms have their  $\tau_{\text{max}}$  eigenvector aligned along the principal direction of  $g_{\text{min}}$ . This reflects the appreciable contribution of the selenium  $p_{\pi}$  orbitals to the SOMO shown in Figure 6.

The spin densities calculated by DFT are given in Table 4. The values predicted for the selenium atoms very well agree

with the EPR spectra; they confirm, for example, that spin delocalization on each selenium atom is slightly smaller for CpNi(bds) than for CpNi(dsit). The same decrease in the spin densities on the two chalcogen atoms is predicted when passing from the dmit to the bdt complex; it is accompanied by an increase in the Ni spin density. A similar spin transfer ( $\sim +10\%$ ) from the chalcogens to the metal occurs when passing from the dithiolene to the corresponding diselenolene complex. The total spin densities on the cyclopentadiene ring, are close to 20% for both CpNi(bds) and CpNi(bdt).

Because DFT calculations are consistent with EPR measurements, at least for the  $g$  tensors and the selenium spin densities, it is worthwhile using optimized structures of the isolated CpNi(bds) and CpNi(bdt) complexes to understand the magnetic properties of these compounds in the crystal state. Consistent with magnetic measurements, the DFT results shown in Table 3 for the idealized dimer or for the exact crystal structure geometry, indicate an antiferromagnetic coupling. All the values of  $J_N$  obtained with GGA functionals are between  $-190$  and  $-290 \text{ cm}^{-1}$  and are quite different from the values obtained with hybrid functionals. The dependence of  $J$  upon the type of functional used for the calculations has been reported in many recent articles.<sup>30,35,37</sup> The absolute value of  $J$  calculated using generalized gradient approximation (GGA) are generally found to be larger than those calculated with hybrid functionals but smaller than with local functionals. Similar variations are observed in Table 3. However, in contrast with the values given in this table, in most of the previous studies a rather good agreement between experiment and calculation was obtained with hybrid functionals, whereas GGA was found to overestimate the antiferromagnetic behavior.<sup>37,38</sup> For the [CpNi(bds)]<sub>2</sub> and the [CpNi(bdt)]<sub>2</sub> systems, the better accord between measured and predicted  $J$  values is obtained by using the BLYP functional. It is difficult to know, for the moment, if this accord is due to some specificities of these systems (e.g., bridge formed by two rings without covalent bonds) or if magnetic interactions with other neighboring CpNi(bds) or CpNi(bdt) units, contributing to the measured  $J$  value. However, due to the large intermolecular chalcogen...chalcogen distances measured on the crystal,<sup>4</sup> this last interpretation seems less probable.

It is important, for the design of new materials, to detect the structural parameters that drive the magnetic properties of a molecular complex. These properties are the outcome among several factors such as hybridization of the various atoms, bond lengths, molecular conformation, ....<sup>39</sup> Due to the axial nature of the Cp...Cp bridge linking the two magnetic moieties in

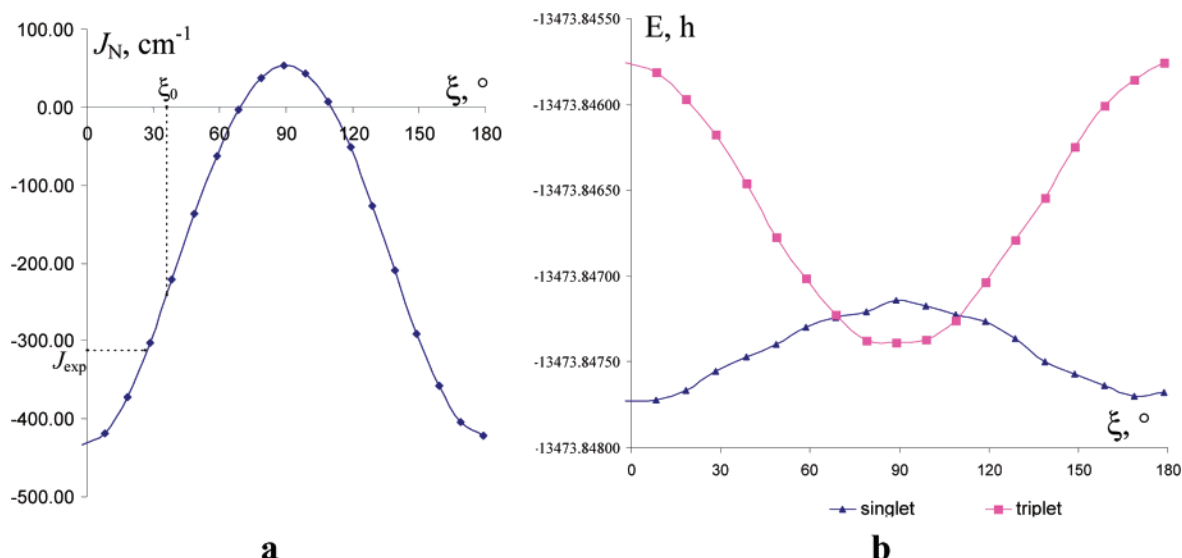


**Figure 5.** (a) Variation of the exchange coupling parameter  $J_N$  with the SeNiNiSe dihedral angle  $\xi$  for (bds)NiCp...CpNi(bds).  $\xi_0$  corresponds to the idealized dimer;  $J_{\text{exp}}$  is the experimental value. (b) Corresponding potential energy surfaces (singlet and triplet) as a function of the SeNiNiSe dihedral angle  $\xi$ . Curves a and b calculated with the BP86 functional.

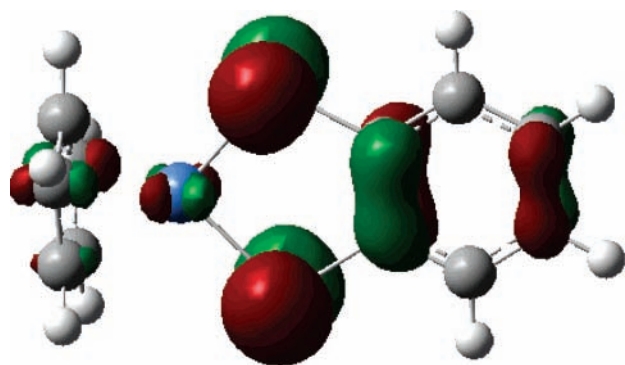


**Figure 6.** Representation of the SOMO for CpNi(bds).

**TABLE 4: Calculated Spin Densities**

	basis set <sup>a</sup>	Se(1)	Se(2)	Ni	C <sub>6</sub> H <sub>6</sub>	C <sub>2</sub> S <sub>2</sub> CS	C <sub>5</sub> H <sub>5</sub>
CpNi(bdt)	set a	0.15	0.15	0.49	0.01		0.20
	set b	0.16	0.16	0.48	0.02		0.18
	set c	0.14	0.15	0.52	0.02		0.17
CpNi(bds)	set a	0.10	0.09	0.60	0.01		0.20
	set b	0.11	0.11	0.58	0.02		0.18
	set c	0.10	0.09	0.62	0.02		0.17
CpNi(dmit)	set a	0.23	0.23	0.29		0.10	0.15
	set b	0.23	0.22	0.29		0.13	0.13
	set c	0.22	0.21	0.33		0.11	0.13
CpNi(dsit)	set a	0.17	0.17	0.45		0.04	0.17
	set b	0.18	0.18	0.42		0.07	0.15
	set c	0.16	0.15	0.48		0.06	0.15

<sup>a</sup> Set a, G03, B3LYP, basis: C, H, S, Se, aug-cc-pVDZ; Ni, SBK. Set b, ORCA, B3LYP, basis: C, H, S, Se, aug-cc-pVDZ; Ni, TZV. Set c, ORCA, B3LYP, basis: C, H, S, Se, aug-cc-pVDZ; Ni, TZV, ZORA.

RNiCp...CpNiR (R = bdt or bds), these “dimers” are specially appropriate to assess the role of the relative orientation of the two Ni(diselenolene) (or dithiolene) planes. The dependence of  $J$  upon the corresponding dihedral angle  $\xi$  is shown in Figure 5 for the bds containing dimer; the value  $\xi_0$  corresponding to the idealized structure is also visualized, together with the experimental value  $J_{\text{exp}}$ . As expected, the maximum of the antiferromagnetic coupling is obtained when the two chalcogen–Ni–chalcogen units (the fragments that, in the monomer, bear the most important part of the spin) are oriented parallel

( $J_{\text{min}} = -430 \text{ cm}^{-1}$ ).<sup>40</sup> However, for a dihedral angle between  $70^\circ$  and  $110^\circ$ , the system is predicted to be ferromagnetic with  $J_{\text{max}}$  equal to  $\sim 60 \text{ cm}^{-1}$ . It is worthwhile mentioning that similar results are obtained for the dimeric structure of CpNi(bdt); in this case; however, the minimum and maximum values of  $J$  are equal to  $-381$  and  $+54 \text{ cm}^{-1}$ , respectively.

## Conclusion

Owing to <sup>77</sup>Se enrichment of CpNi(diselenolene), the  $g$  tensor as well as the <sup>77</sup>Se hyperfine tensors of these complexes could be measured from their frozen solution EPR spectra. They reasonably agree with those calculated by DFT. This accord corroborates the spin distribution found by DFT ( $\sim 10\%$  on each selenium and  $\sim 19\%$  on the cyclopentadiene ring). This spin delocalization on the cyclopentadienyl rings is expected to give rise to unresolved proton couplings and explains, at least in part, the broadening of the EPR lines. The exchange coupling parameter  $J$  calculated for the idealized dimeric structure is consistent with the experimental value, but it also strongly depends upon the dihedral angle between the two diselenolene planes.

**Acknowledgment.** We gratefully acknowledge support from Swiss National Foundation and from the “Fonds Germaine de Staël” (Schweizerische Akademie der Technischen Wissenschaften and French Ministry of Foreign Affairs).

**Supporting Information Available:** Variation of the exchange coupling parameter  $J_N$  and of the singlet and triplet energies with the SNiNiS dihedral angle for (bdt)CpNi...NiCp(bdt). This material is available free of charge via the Internet at <http://pubs.acs.org>.

## References and Notes

- (1) Geiger, W. E.; Allen, C. S.; Mines, T. E.; Senftleber, F. C. *Inorg. Chem.* **1977**, *16*, 2003.
- (2) Bowmaker, G. A.; Boyd, P. D.; Campbell, G. K. *Inorg. Chem.* **1983**, *22*, 1208.
- (3) Bowmaker, G. A.; Boyd, P. D.; Zvagulis, M.; Cavell, K. J. *Inorg. Chem.* **1985**, *24*, 401.
- (4) Nomura, M.; Cauchy, T.; Geoffroy, M.; Adkine, P.; Fourmigué, M. *Inorg. Chem.* **2006**, *45*, 8194.
- (5) Fourmigué, M.; Avarvari, N. *J. Chem. Soc., Dalton Trans.* **2005**, 1365.

- (6) Nomura, M.; Geoffroy, M.; Adkine, P.; Fourmigué, M. *Eur. J. Inorg. Chem.* **2006**, 5012.
- (7) Nomura, M.; Fourmigué, M. *New J. Chem.* **2007**, 31, 528.
- (8) Cauchy, T.; Ruiz, E.; Jeannin, O.; Nomura, M.; Fourmigué, M. *Chem. Eur. J.* **2007**, 13, 8858.
- (9) Hanson, G. H.; Gates, K. E.; Noble, C. J.; Griffin, M.; Mitchell, A.; Benson, S. J. *Inorg. Biochem.* **2004**, 98, 903.
- (10) Soulié, E. J.; Berclaz, T. *Appl. Magn. Reson.* **2005**, 29, 401.
- (11) Frisch, M. J.; Trucks, G. W.; Schlegel, H. B.; Scuseria, G. E.; Robb, M. A.; Cheeseman, J. R.; Montgomery, J. A., Jr.; Vreven, T.; Kudin, K. N.; Burant, J. C.; Millam, J. M.; Iyengar, S. S.; Tomasi, J.; Barone, V.; Mennucci, B.; Cossi, M.; Scalmani, G.; Rega, N.; Petersson, G. A.; Nakatsuji, H.; Hada, M.; Ehara, M.; Toyota, K.; Fukuda, R.; Hasegawa, J.; Ishida, M.; Nakajima, T.; Honda, Y.; Kitao, O.; Nakai, H.; Klene, M.; Li, X.; Knox, J. E.; Hratchian, H. P.; Cross, J. B.; Adamo, C.; Jaramillo, J.; Gomper, R.; Stratmann, R. E.; Yazyev, O.; Austin, A. J.; Cammi, R.; Pomelli, C.; Ochterski, J. W.; Ayala, P. Y.; Morokuma, K.; Voth, G. A.; Salvador, P.; Dannenberg, J. J.; Zakrzewski, V. G.; Dapprich, S.; Daniels, A. D.; Strain, M. C.; Farkas, O.; Malick, D. K.; Rabuck, A. D.; Raghavachari, K.; Foresman, J. B.; Ortiz, J. V.; Cui, Q.; Baboul, A. G.; Clifford, S.; Cioslowski, J.; Stefanov, B. B.; Liu, G.; Liashenko, A.; Piskorz, P.; Komaromi, I.; Martin, R. L.; Fox, D. J.; Keith, T.; Al-Laham, M. A.; Peng, C. Y.; Nanayakkara, A.; Challacombe, M.; Gill, P. M. W.; Johnson, B.; Chen, W.; Wong, M. W.; Gonzalez, C.; Pople, J. A. *Gaussian 03*, revision B.03; Gaussian, Inc.: Pittsburgh, PA, 2003.
- (12) (a) Becke, A. D. *J. Chem. Phys.* **1986**, 84, 4524. (b) Becke, A. D. *J. Chem. Phys.* **1993**, 98, 5648. (c) Lee, C. T.; Yang, W. T.; Parr, R. G. *Phys. Rev. B* **1988**, 37, 785.
- (13) (a) Krishnan, R.; Binkley, J. S.; Seeger, R.; Pople, J. A. *J. Chem. Phys.* **1980**, 72, 650. (b) Blaudeau, J.-P.; McGrath, M. P.; Curtiss, L. A.; Radom, L. *J. Chem. Phys.* **1997**, 107, 5016. (c) Curtiss, L. A.; McGrath, M. P.; Blandeau, J.-P.; Davis, N. E.; Binning, R. C., Jr.; Radom, L. *J. Chem. Phys.* **1995**, 103, 6104.
- (14) Stevens, W. W. J.; Krauss, M.; Basch, H.; Jasien, P. G. *Can. J. Chem.* **1992**, 70, 612.
- (15) (a) Dunning, T. H., Jr. *J. Chem. Phys.* **1989**, 90, 1007. (b) Kendall, R. A.; Dunning, T. H., Jr.; Harrison, R. J. *J. Chem. Phys.* **1992**, 96, 6796. (c) Woon, D. E.; Dunning, T. H., Jr. *J. Chem. Phys.* **1993**, 98, 1358. (d) Wilson, A. K.; Woon, D. E.; Peterson, K. A.; Dunning, T. H., Jr. *J. Chem. Phys.* **1999**, 110, 7667.
- (16) (a) Neese, F. *J. Chem. Phys.* **2001**, 115, 11080. (b) Neese, F. ORCA – an ab initio, Density Functional and Semiempirical program package, Version 2.5. University of Bonn, 2006.
- (17) (a) Schäfer, A.; Horn, H.; Ahlrichs, R. *J. Chem. Phys.* **1992**, 97, 2571. (b) Schafer, A.; Huber, C.; Ahlrichs, R. *J. Chem. Phys.* **1994**, 100, 5829.
- (18) Van Lenthe, E.; Baerends, E. J.; Snijders, J. *J. Chem. Phys.* **1993**, 99, 4597.
- (19) van Wüllen, C. *J. Chem. Phys.* **1998**, 109, 392.
- (20) Perdew, J.; Burke, K.; Ernzerhof, M. *Phys. Rev. Lett.* **1996**, 77, 3685.
- (21) Faulmann, C.; Delpech, F.; Malfant, L.; Cassoux, P. *J. Chem. Soc., Dalton Trans.* **1996**, 2261.
- (22) Nomura, M.; Okuyama, R.; Fujita-Tayakama, C.; Kajitani, M. *Organometallics* **2005**, 24, 5110.
- (23) Neese, F. *J. Chem. Phys.* **2001**, 115, 11080.
- (24) Mattar, S. M. *J. Phys. Chem. A* **2007**, 111, 251.
- (25) Patchkovskii, S.; Ziegler, T. *J. Phys. Chem. A* **2001**, 105, 5490.
- (26) Saladino, A. C.; Larsen, S. C. *Catal. Today* **2005**, 105, 122.
- (27) Noodleman, L. *J. Chem. Phys.* **1981**, 74, 5737.
- (28) Noodleman, L.; Davidson, E. R. *J. Chem. Phys.* **1986**, 109, 131.
- (29) Cano, J.; Rodriguez-Fortea, A.; Alemany, P.; Alvarez, S.; Ruiz, E. *Chem. Eur. J.* **2000**, 6, 327.
- (30) Noh, E. A. A.; Zhang, J. *J. Chem. Phys.* **2006**, 330, 82.
- (31) Mattar, S. M. *J. Chem. Phys. Lett.* **2006**, 427, 438.
- (32) Cramer, C. J. *Essentials of Computational Chemistry*; John Wiley: Chichester, U.K., 2004.
- (33) Neese, F. *J. Phys. Chem. Solids* **2004**, 65, 781.
- (34) Yamaguchi, K.; Takahara, Y.; Fueno, T. In *Applied Quantum Chemistry*; Smith, V. H., Ed.; **Chemistry**; Reidel: Dordrecht, The Netherlands, 1986.
- (35) Illas, F.; Moreira, I. de P. R.; Bofill, J. M.; Filatov, M. *Theor. Chem. Acc.* **2006**, 116, 587.
- (36) Morton, J. R.; Preston, K. F. *J. Magn. Reson.* **1978**, 30, 577.
- (37) Wang, B.; Wei, H.; Wang, M.; Chen, Z. *J. Chem. Phys.* **2005**, 122, 204310.
- (38) Sinneker, S.; Neese, F.; Noodleman, L.; Lubitz, W. *J. Am. Chem. Soc.* **2004**, 126, 2613.
- (39) Andriotis, A. N.; Lathiotakis, N. N.; Menon, M. *Europhys. Lett.* **1996**, 36, 37.
- (40) (a) Kahn, O. *Molecular Magnetism*; VCH: New York, 1993. (b) Amabilino, D.; Veciana, J. In *Magnetism: Molecules to Materials II*; Miller, J. S., Drillon, M., Eds.; Wiley-VCH: Weinheim, 2001. (c) Dougherty, D. A. *Acc. Chem. Res.* **1991**, 24, 88.